Am J Transl Res 2022;14(7):5155-5163
www.ajtr.org /ISSN:1943-8141/AJTR0143727

Original Article

Biomechanical effect of Coflex and X-STOP spacers on the lumbar spine: a finite element analysis

Zhiyuan Guo, Guangfei Liu, Lu Wang, Yuejiang Zhao, Ye Zhao, Shouliang Lu, Cai Cheng

Department of Orthopedics, Cangzhou Central Hospital, Cangzhou, Hebei, China

Received April 24, 2022; Accepted June 9, 2022; Epub July 15, 2022; Published July 30, 2022

Abstract: Objective: To explore the biomechanical differences between Coflex and X-STOP devices by finite element analysis. Methods: Based on the normal lumbar CT images from a healthy adult volunteer, four finite element models including the healthy lumbar segment model, the mild degenerated lumbar segment model, a Coflex fixed lumbar segment model and X-STOP fixed lumbar segment model were constructed. A simulation analysis under the conditions of flexion, extension, lateral bending, and rotation was performed to compare range of motion (ROM), intradiscal pressure, the facet joint force, the maximum Von Mises stress and the peak facet contact forces, between Coflex and X-STOP devices. Results: Compared to the mild degenerated lumbar segment model at surgical level L4-L5, Coflex and X-STOP could reduce ROM in extension by 98.34% and 95.86%, respectively, decrease peak stress of intervertebral discs in extension by 59.4% and 66.17%, respectively, and release peak force of facet joint in extension by 97.09% and 95.42%, respectively. Both devices had no significant impact on adjacent levels. The maximum Von Mises stress in Coflex device was 637.56 Mpa in flexion, 528.86 Mpa in extension, while the maximum Von Mises stress in X-STOP device was 476.65 Mpa at extension position. The peak facet contact forces of Coflex and X-STOP devices appeared in extension and were 19.76 Mpa and 49.28 Mpa, respectively. Conclusions: Coflex and X-STOP devices can effectively decrease the ROM and intradiscal pressure in extension, without affecting the adjacent levels.

Keywords: Coflex, X-STOP, finite element analysis, biomechanical properties, lumbar vertebrae

Introduction

With the aging population, low back and leg pain caused by lumbar spinal degenerative diseases, including lumbar disc herniation, lumbar spinal stenosis, and lumbar spondylolisthesis, seriously affect the patients' quality of life [1, 2]. In clinical practice, for patients with lumbar spinal degenerative diseases, spinal fusion is a common treatment, especially for potential deformity or instability. However, spinal fusion can exert adverse effects on adjacent segments such as increased interspinous pressure and limited range of motion (ROM), which are also correlated with nonunion, pseudarthrosis, and instrumentation failure [3]. Currently, dynamic stabilization, as an alternative method, is used increasingly. Some studies revealed that dynamic stabilization could indirectly realize the decompression, limit extension, expand the spinal canal, and restrict the stress in the intervertebral discs [4, 5]. Other studies showed that dynamic stabilization could achieve the same postoperative outcome with lower incidence of complications in contrast to spinal fusion [6, 7].

In recent years, Coflex and X-STOP, as interspinous process devices, have been used for the treatment of lumbar spinal degenerative diseases with different designs of biomechanics [8, 9]. Some studies found that compared to instrumented fusion, better outcomes including a higher success rate were observed in decompression using a Coflex device [10]. Other studies reported that Coflex and X-STOP devices could strongly decrease and stabilize the intradiscal pressure and have little impact on other motion modes. Park et al. investigated the pretension effects of ligature on spinous process fracture in Coflex and X-STOP device implantation [11]. Moreover, the application and effectiveness of Coflex and X-STOP were also ques-

Table 1. Properties of material in the finite element model

Component	Young Modulus (Mpa)	Poisson ratio	Cross-sectional area (mm^2)
Cortical bone	12000	0.3	
Trabecular bone	100	0.2	
End-plates	3000	0.25	
Posterior element	3500	0.25	
Cartilago articularis	25	0.4	
Annulus ground substance	4.2	0.45	
Nucleus pulpous	1	0.499	
Anterior longitudinal ligaments	20	0.3	40
Posterior longitudinal ligaments	20	0.3	20
Ligamentum flavum	19.5	0.3	40
Supraspinous ligament	15	0.3	40
Interspinous ligament	12	0.3	30
Intertransverse ligament	59	0.3	10
Capsular ligaments	32.9	0.3	30

tioned [10, 12]. The effect of the different biomechanical designs of Coflex and X-STOP on the stability of the lumbar spine, interspinous pressure, and stress of a facet joint are not clearly understood. Therefore, careful evaluation of biomechanical properties of Coflex and X-STOP is required to confirm the effectiveness and avoid complications.

In this study, the biomechanical characteristics of different interspinous spacers were analyzed with the finite element method. Coflex and X-STOP devices were chosen in the present study. The results of this study will guide the strategy of treatment for these patients in need of dynamic stabilization.

Materials and methods

Construction of finite element model for healthy lumbar spine

The geometry of the lumbosacral spine was constructed by computerized tomographic (CT) scans of a healthy adult (37 years old, 160 cm in height and 55 kg in weight). Mimics software version 20.0 (Materialise Company, Belgium) was used to transform the CT images into a 3-D geometric model, which was meshed by Hypermesh software (Altair Technologies Company, USA). Geomagic I2.0 (Geomagic Company, USA), Solidworks 2015 (Dassault Company, France) and Ansys Workbench 18.0 (Ansys Company, USA) were exploited to develop the lumbar spine model. The final finite element model included a vertebral body, intervertebral disc, end-plate, facet joint, and seven kinds of ligaments. The vertebral body consisted of inner trabecular bone and outer cortical bone 1 mm thick. 1 mm thick end-plates covered the inferior and superior surfaces of the vertebral body. The intervertebral disc is made of nucleus pulposus and annulus fibrosus. The volume of the nucleus pulposus accounts for about 50% of the intact intervertebral disc with the modulus elasticity of 1 Mpa. The annulus fibrosus was developed with eight layers and modeled as truss elements. The facet joint contacts were modeled as surface-to-surface contact elements without friction. There were 310493 nodes and 110457 elements included in the finite element model of healthy lumbar spine. These ligaments were modeled as tension-only truss elements. The characteristics of all elements are shown in **Table 1**. This study was approved by the Ethics Committee of Cangzhou Central Hospital (No. 2020-118).

Construction of finite element model for mild degenerated lumbar spine

Based on the finite element model of healthy lumbar spine and the criterion proposed by Wilkes et al. [13], the intervertebral disc was deformed and the height of the intervertebral space in mild degenerated intervertebral disc was decreased by 16.5% and the volume of nucleus pulposus accounted for 60% of the intact intervertebral disc. According to the report by Natarajan et al. [14], the material properties of the nucleus pulposus and annulus fibrosis were modified. Compared to normal intervertebral discs, the elastic modulus of the nucleus pulposus and annulus fibrosis in mildly degenerated intervertebral discs becomes increased by 1.16 and 4.8 times, respectively, and the Poisson's ratio is decreased to varying degrees.

Coflex and X-STOP fixed L4-L5 segment models

Before implantation, the interspinous ligaments and supraspinous ligaments were resected. The geometry of Coflex and X-STOP devices were established according to the real

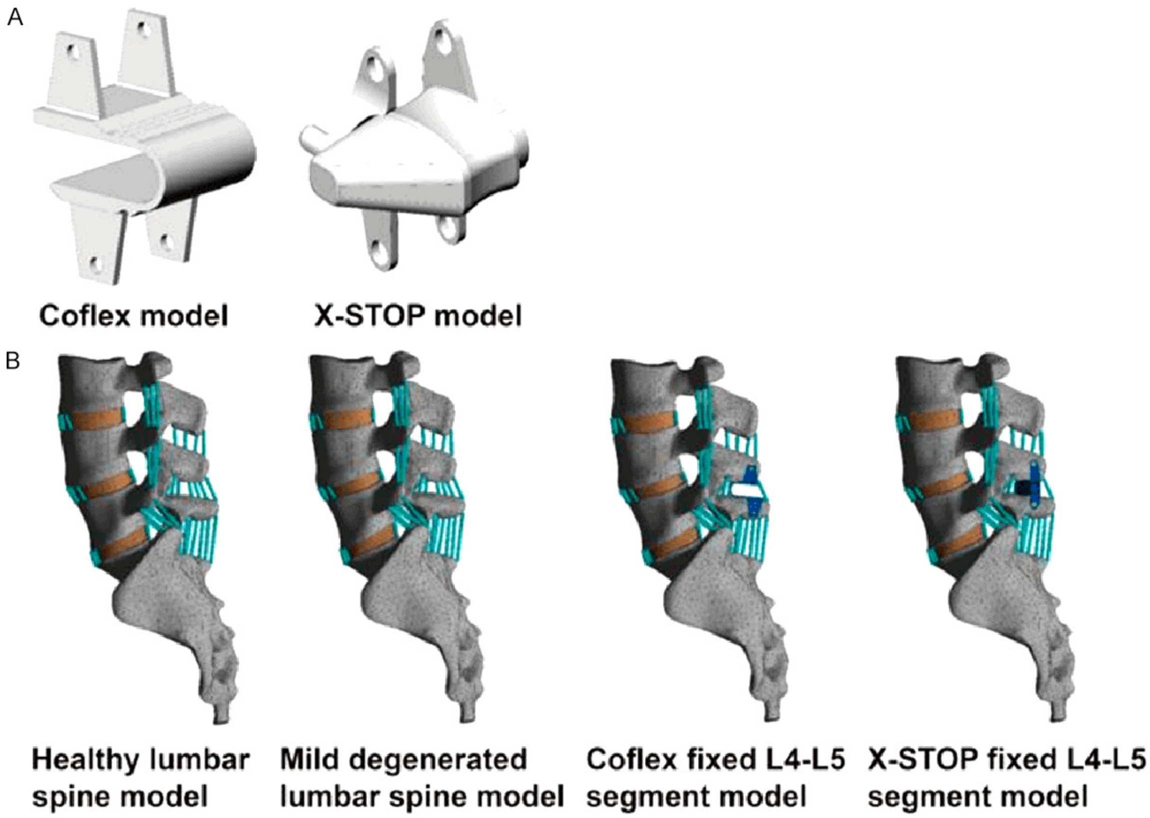

Figure 1. 3-D geometry models with interspinous spacers. A: Coflex and X-STOP devices. B: Different kinds of lumbar spine models.

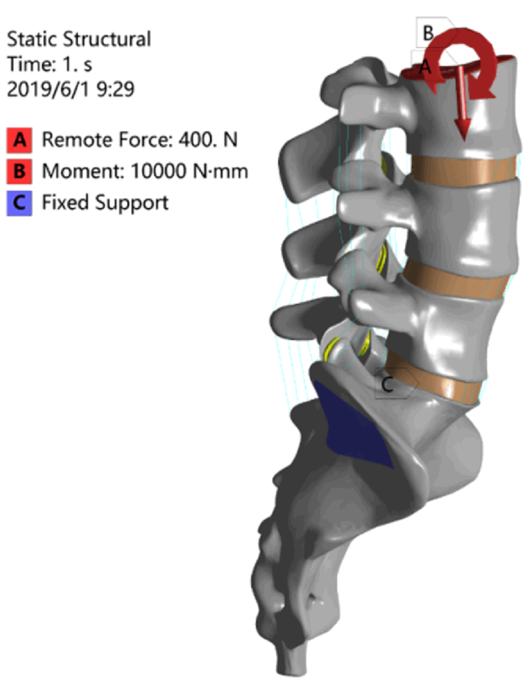

Figure 2. Schematic of flexion loading.

product. The mildly degenerated model was modified to insert Coflex or X-STOP into the interspinous space L4/L5, independently. The surface between the interspinous space and bony tissues was considered as surface-to-surface contact. The coefficient of friction was set to 0.8 for the wing contacting the spinous process, while the coefficient of friction was set to 0.1 for other contact regions. The models of Coflex and X-STOP were validated by an experienced operator, as shown in **Figure 1**.

Loading and boundary conditions

In all the finite elemental models, the bottom surface of the L5 vertebra was constrained. The compressive load was simulated by a two-node link element which attached near the geometric center in each vertebra and kept a tangent following the curve of the spine. According to a previous study [15], a compressive load of 400 N and 10 Nm of momentum were imposed by contracting the link elements to simulate the real physiologic activities, as seen in **Figure 2**.

Table 2. Results regarding intersegmental ROMs of healthy lumbar segment model

Segment	ROM (°)			
	Flexion	Extension	Lateral bending	Axial rotation
L2-L3	3.36	3.58	3.21	1.85
L3-L4	6.05	4.29	3.67	1.86
L4-L5	5.86	4.47	2.84	1.75

Under the conditions of this compression, the flexion, extension, lateral bending, and rotation were generated. In the present study, ROM, peak force of facet joint, intradiscal pressure, facet joint force, the peak facet contact forces, and maximum Von Mises stress were detected in these four motions. Moreover, the effects of interspinous spacers on the adjacent segments were examined by a hybrid testing protocol reported by Fan et al. [16].

Statistical analyses

Clinical data included in this study were analyzed by SPSS statistical software package (Version 20.0; IBM Corporation, United States). The enumerated data were expressed by number or percentage. The measured data were presented as mean ± standard deviation.

Results

Validation of a healthy segment model

The intersegmental ROMs of healthy lumbar segment model in term of flexion, extension, lateral bending, and axial rotation are shown in **Table 2**. These ROM results observed from the healthy lumbar segment model were similar to those in a previous study [17]. The difference between the present study and the study of Xiao et al. [17] was within 5%, which was due to the subjects used in the design of the models. Those results also indicated that the healthy lumbar segment model in this study was successfully developed and could be applied for further modeling and analysis.

Range of motion

At the operative level L4-L5, the results of ROMs from the mildly degenerated lumbar segment model and interspinous spacers fixed lumbar segment model were normalized with respect to the healthy lumbar segment model. As shown in **Table 3**, compared to the mildly degenerated lumbar segment model, the ROMs in the Coflex fixed lumbar segment model was decreased by 24.44% in flexion, 98.34% in extension, 12.90% in left lateral bending, 9.29% in right lateral bending, 23.74% in left rotation, and 21.88% in right rotation, while those in the X-STOP fixed lumbar segment model were decreased by 32.02% in flexion, 95.86% in extension, 17.92% in left lateral bending, 17.14% in right lateral bending, 26.07% in left rotation, and 26.56% in right rotation.

At adjacent level L3-L4, in contrast to the mildly degenerated lumbar segment model, the the ROM in Coflex fixed lumbar segment model was decreased by 11.01% in flexion, 17.06% in extension, 24.01% in left lateral bending, 1.74% in right lateral bending, 2.58% in left rotation, and 2.22% in right rotation. The ROM in the X-STOP fixed lumbar segment model was decreased by 13.46% in flexion, 17.66% in extension, 25.11% in left lateral bending, 3.27% in right lateral bending, 3.69% in left rotation, and 1.48% in right rotation.

At adjacent level L5-S1, compared to the mildly degenerated lumbar segment model, the ROM in Coflex fixed lumbar segment model was decreased by 6.95% in flexion, 11.81% in extension, 2.13% in left lateral bending, 1.72% in right lateral bending, 3.29% in left rotation, and 3.21% in right rotation. The ROM in the X-STOP fixed lumbar segment model was decreased by 3.23% in flexion, 10.07% in extension, 1.70% in left lateral bending, 1.29% in right lateral bending, 5.16% in left rotation, and 3.19% in right rotation.

Intradiscal pressure

As shown in **Table 4**, at the operative level L4-L5, compared to the mildly degenerated lumbar segment model, the peak stress of intervertebral discs in the Coflex fixed lumbar segment model was decreased by 27.62% in flexion, 59.40% in extension, 10.33% in left lateral bending, 7.45% in right lateral bending, 6.48% in left rotation and 4.67% in right rotation. The peak stress of intervertebral discs in X-STOP fixed lumbar segment model was decreased by 29.83% in flexion, 66.17% in extension, 18.48% in left lateral bending, 19.15% in right lateral bending, 11.11% in left rotation and 9.35% in right rotation.

Table 3. Results of range of motion in the mildly degenerated lumbar segment model and interspinous spacers fixed lumbar segment model

Dynamic	ROM/(°)				
	Mildly degenerated model	Coflex	Percentage of decrease	X-STOP	Percentage of decrease
Flexion	3.56	2.69	24.44%	2.42	32.02%
Extension	3.62	0.06	98.34%	0.15	95.86%
Left lateral bending	2.79	2.43	12.90%	2.29	17.92%
Right lateral bending	2.80	2.54	9.29%	2.32	17.14%
Left rotation	2.57	1.96	23.74%	1.90	26.07%
Right rotation	2.56	2.00	21.88%	1.88	26.56%

Table 4. Results of the peak stress of intervertebral discs in the mildly degenerated lumbar segment model and interspinous spacers fixed lumbar segment model

Dynamic	Peak stress of intervertebral discs (Mpa)				
	Mildly degenerated model	Coflex	Percentage of decrease	X-STOP	Percentage of decrease
Flexion	1.81	1.31	27.62%	1.27	29.83%
Extension	1.33	0.54	59.40%	0.45	66.17%
Left lateral bending	1.84	1.65	10.33%	1.50	18.48%
Right lateral bending	1.88	1.74	7.45%	1.52	19.15%
Left rotation	1.08	1.01	6.48%	0.96	11.11%
Right rotation	1.07	1.02	4.67%	0.97	9.35%

Table 5. Results of peak force of the facet joint in the mildly degenerated lumbar segment model and interspinous spacers fixed lumbar segment model

Dynamic	Peak force of facet joint (Mpa)				
	Mildly degenerated model	Coflex	Percentage of decrease	X-STOP	Percentage of decrease
Flexion	1.35	1.26	6.67%	1.16	14.07%
Extension	8.95	0.26	97.09%	0.41	95.42%
Left lateral bending	4.52	3.88	14.16%	3.42	24.34%
Right lateral bending	5.01	4.07	18.76%	3.35	33.13%
Left rotation	7.51	4.18	44.34%	1.10	85.35%
Right rotation	7.04	4.27	39.35%	2.92	58.52%

At adjacent level L3-L4, in contrast to the mildly degenerated lumbar segment model, the peak stress of intervertebral discs in the Coflex fixed lumbar segment model was increased by 1.09% in flexion, 20.62% in extension, 0.10% in left rotation and 0.15% in right rotation, and decreased by 7.64% in left lateral bending and 6.22% in right lateral bending. The peak stress of intervertebral discs in the X-STOP fixed lumbar segment model was increased by 11.94% in flexion, 22.04% in extension, and 0.09% in left rotation, and decreased by 7.89% in left lateral bending, 6.05% in right lateral bending, and 0.52% in right rotation.

At adjacent level L5-S1, compared to the mildly degenerated lumbar segment model, the peak stress of intervertebral discs in the Coflex fixed lumbar segment model was increased by 0.78% in flexion, 0.17% in left rotation and 0.27% in right rotation, and decreased by 24.71% in extension, 3.05% in left lateral bending, 6.37% in right lateral bending. The peak stress of intervertebral discs in the X-STOP fixed lumbar segment model was increased by 7.00% in flexion and 5.27% in left rotation, and decreased by 22.24% in extension, 0.08% in left lateral bending, 5.32% in right lateral bending, and 0.41% in right rotation.

Facet joint force

The facet joint force at the surgical level L4-L5 is shown in **Table 5**. Compared to the mildly

Table 6. Results of maximum Von Mises stress in interspinous spacers fixed lumbar segment model

Dynamic	maximum Von Mises stress (Mpa)	
	Coflex	X-STOP
Flexion	637.56	≈0
Extension	528.86	476.65
Lateral bending	18.47	158.94
Rotation	129.95	≈0

Table 7. Results of peak facet contact forces in the interspinous spacers fixed lumbar segment model

Dynamic	Peak facet contact force (Mpa)	
	Coflex	X-STOP
Flexion	0	0
Extension	19.76	49.28
Lateral bending	5.92	29.84
Rotation	1.26	0

degenerated lumbar segment model, the peak force of the facet joint in Coflex fixed lumbar segment model was decreased by 6.67% in flexion, 97.09% in extension, 14.16% in left lateral bending, 18.76% in right lateral bending, 44.34% in left rotation, and 39.35% in right rotation. The peak force of facet joint in the X-STOP fixed lumbar segment model was decreased by 14.07% in flexion, 95.42% in extension, 24.34% in left lateral bending, 33.13% in right lateral bending, 85.35% in left rotation, and 58.52% in right rotation.

In contrast to the mild degenerated lumbar segment model at adjacent level L3-L4, the peak force of facet joint in the Coflex fixed lumbar segment model was decreased by 6.23% in flexion, 38.13% in extension, 17.15% in left lateral bending, and increased by 76.57% in right lateral bending, 4.23% in left rotation, and 31.94% in right rotation.

The peak force of the facet joint in X-STOP fixed lumbar segment model was increased by 20.25% in flexion, 7.41% in left lateral bending, 42.83% in right lateral bending, 22.75% in left rotation and 19.71% in right rotation, and decreased by 43.52% in extension.

Compared to the mild degenerated lumbar segment model at adjacent level L5-S1, the peak force of facet joint in the Coflex fixed lumbar segment model was increased by 47.66% in extension, 0.84% in left rotation, and 1.74% in right rotation, and decreased by 3.43% in flexion, 5.85% in left lateral bending and 3.66% in right lateral bending. The peak force of facet joint in the X-STOP fixed lumbar segment model was decreased by 1.24% in flexion, 6.57% in left lateral bending and 19.35% in right rotation, and increased by 17.44% in extension, 0.57% in right lateral bending, and 51.59% in left rotation.

Maximum Von Mises stress

As shown in **Table 6**, the maximum Von Mises stress of the Coflex device at surgical level L4-L5 was 637.56 Mpa in flexion, 528.86 Mpa in extension, 129.95 Mpa in rotation and 18.47 Mpa in lateral bending. Whereas, the maximum Von Mises stress of X-STOP device at surgical level L4-L5 was 476.65 Mpa in extension, and 158.94 Mpa in lateral bending. The maximum stress of X-STOP device was almost 0 in flexion and rotation. Under these conditions, X-STOP device was subjected to no load.

The peak facet contact forces

As shown in **Table 7**, the peak facet contact forces of the Coflex device at surgical level L4-L5 was 19.76 Mpa in extension, 5.92 Mpa in lateral bending and 1.26 Mpa in rotation. The peak facet contact force of the Coflex device in flexion was 0. The peak facet contact forces of X-STOP device at surgical level L4-L5 was 49.28 Mpa in extension and 29.84 Mpa in lateral bending. The peak facet contact forces of X-STOP device were 0 in flexion and rotation.

Discussion

WALLIS, as the first interspinous device, was introduced in 1986 [18]. Since that, a large number of interspinous devices were developed and popularized in clinical practice. The interspinous devices were designed to be implanted into the space between the adjacent spinous processes. The aim of these interspinous spacers is to maintain the stability following relieving the compression of nerves at the surgical segment levels [19]. In recent years, the interspinous devices were considered as an alternative to decompression alone, or instrumented fusion, either in combination with decompression or as a stand-alone device.

However, until now, to the best of our knowledge, few studies have been performed to evaluate the biomechanical properties of these interspinous spacers and there was still a lack of biomechanical data for interspinous devices.

In the present finite element analysis, we comprehensively evaluated the biomechanical effects of the interspinous soft fixation with Coflex or X-STOP at the segments of L4-L5. The results showed that Coflex or X-STOP devices were not responsible for the intradiscal pressure at the adjacent segments. Coflex or X-STOP implanted into L4-L5 segment could generate a reduced force on the facet joint and the posterior part of the intervertebral disc during extension. In term of ROM, Coflex or X-STOP implants could decrease ROM during extension and had no impact on ROM at the adjacent segment levels. The peak facet contact forces in Coflex or X-STOP models were in extension. However, the maximum Von Mises stress in the Coflex model was in flexion, while the maximum Von Mises stress in the X-STOP model was in extension.

Stimulation of the sinuvertebral nerve in posterior annulus and medial branches in facet joints could lead to pain in lumbar spinal degenerative diseases. It was reported that the reduced stress on the facet joint and load on the posterior annulus could relieve pain following surgery to a certain degree. In this study, Coflex and X-STOP devices were found to reduce intradiscal pressure during extension in the posterior annulus. Moreover, according to this study, the effect of the Coflex device on limiting the motions of spine was considered to preserve stability of the spine, and little impact on the adjacent segments could decrease the chance of adjacent segments degeneration. These results were consistent with the results of cadaver studies reported by Wike et al. [20] and the results of finite element analysis revealed by Pan [21]. Although the fixation method of Coflex was similar to the posterior interbody fusion, combining with the relaxation of the annulus fibrosis and almost all ligaments, the Coflex device could decrease the mobility of the adjacent segments and improve the stiffness of the adjacent segments. In the Coflex model, peak stress of intervertebral discs at surgical L4-L5 level was significantly reduced in extension and had little change during flexion, lateral bending, or rotation. For the adjacent segments, the little change of peak stress of intervertebral discs was observed in the Coflex model during four kinds of motions. In addition, the peak stress in the Coflex model appeared at the bottom of the U-shaped place, especially in flexion and extension, while the peak stress was small during lateral bending and rotation. At the same time, maximum Von Mises stress appeared in flexion and extension, while maximum Von Mises stress was relatively small in lateral bending and rotation. These results were similar to reports in previous studies [22].

In cadaveric experiments, the X-STOP spacer only limited the ROM in flexion and extension at surgical segments, and the ROM in the axial torsion and lateral bending were not affected [23], which is almost the same as the results observed in this study. Huang et al. reported that X-STOP had little effect on the height of intervertebral disc and sagittal motions in adjacent segments [24], which was also similar to the results in this finite element analysis. During flexion and rotation, the increased distance between the upper and lower spinous processes could lead to the separation of the X-STOP device from the upper and lower spinous processes. Under these conditions, X-STOP was in an unstable state and was kept at the original location only depending on interspinous ligament and both of wings. Some studies reported that the interspinous ligament was often resected by a surgeon, causing easier slippage of the X-STOP device [25]. During extension, the decreased distance between the upper and lower spinous process could compress the X-STOP device, and generating greater stress on the contact surface, which could result in a spinous process fracture, especially in these patients with osteoporosis [26]. The peak facet contact forces and maximum Von Mises stress usually appeared at the connection between left wing and screw during extension and lateral bending in the X-STOP model. As we can see, in order to ensure the safety and effectiveness of implants and bone, the motions of extension and lateral bending had to be reduced after surgery. During the surgery, surgeons should strictly follow the surgical procedures, and interspinous ligaments and supraspinous ligaments should beretained as soon as possible.

There are some shortcomings in the present study. First, only the L4/L5 single level was developed and simulated. Other segment levels were not investigated. Second, compared to the healthy disc, different degrees of disc degeneration can cause larger annulus stress and ROM, which was not analyzed in this study. Third, the included data were observed from computerized finite element model simulations, and not from actual measurement observed from cadaveric research. Fourth, the degenerative changes of lumbar spines were not simulated in this finite element analysis. Fifth, the muscles tissues were not considered, and ligaments were simplified in this study. But the proper biomechanical characteristics of muscles tissues and ligaments existed in cadaveric experiments. Further studies are required to determine the effects of interspinous spacers on the lumbar spine.

In summary, in this research, the biomechanical properties of Coflex and X-STOP were explored through simulating the degenerated intervertebral disc model using finite element analysis. The results revealed that Coflex and X-STOP devices could retain most of the ROM in surgical segment levels, maintain the stability of lumbar spinal segments, and reduce intradiscal pressure. Moreover, no significant differences were observed in ROM and intradiscal pressure at the adjacent segment levels before and after implantation of Coflex or X-STOP devices, which indicated that the interspinous spacers played an important role in relieving or avoiding the degeneration at the adjacent segment levels. This suggests that Coflex and X-STOP devices had better biomechanical characteristics and could become an effective and alternative method for spinal fusion treatment or conservative therapy. In addition, the model developed in this study can be exploited not only for simulating and analyzing a single implant, but also for comparison among different types and models of implants at a single segment level in future studies.

Acknowledgements

This research is supported by the Key R&D Program of Hebei Province (No. 182777212).

Disclosure of conflict of interest

None.

Address correspondence to: Cai Cheng, Department of Orthopedics, Cangzhou Central Hospital, No. 16 Xinhua West Road, Cangzhou 061000, Hebei, China. Tel: +86-0317-2075521; Fax: +86-0317-2075521; E-mail: chengcai_edu_cz@163.com

References

[1] He LM, Chen KT, Chen CM, Chang Q, Sun L, Zhang YN, Chang JJ and Feng HY. Comparison of percutaneous endoscopic and open posterior lumbar interbody fusion for the treatment of single-segmental lumbar degenerative diseases. BMC Musculoskelet Disord 2022; 23: 329.

[2] Chu PL, Wang T, Zheng JL, Xu CQ, Yan YJ, Ma QS, Meng-Chen Y and Da-Sheng T. Global and current research trends of unilateral biportal endoscopy/biportal endoscopic spinal surgery in the treatment of lumbar degenerative diseases: a bibliometric and visualization study. Orthop Surg 2022; 14: 635-643.

[3] Li JQ, Sun YP, Guo L, Zhang F, Ding WY and Zhang W. Efficacy and safety of a modified lateral lumbar interbody fusion in L4-5 lumbar degenerative diseases compared with traditional XLIF and OLIF: a retrospective cohort study of 156 cases. BMC Musculoskelet Disord 2022; 23: 217.

[4] Heo M, Yun J, Kim H, Lee SS and Park S. Optimization of a lumbar interspinous fixation device for the lumbar spine with degenerative disc disease. PLoS One 2022; 17: e0265926.

[5] Angelini A, Baracco R, Procura A, Nena U and Ruggieri P. Lumbar stabilization with DSS-HPS((R)) system: radiological outcomes and correlation with adjacent segment degeneration. Diagnostics (Basel) 2021; 11: 1891.

[6] Fuster S, Martinez-Anda JJ, Castillo-Rivera SA, Vargas-Reveron C and Tornero E. Dynamic fixation techniques for the prevention of adjacent segment disease: a retrospective controlled study. Asian Spine J 2022; 16: 401-410.

[7] Peng BG and Gao CH. Is Dynesys dynamic stabilization system superior to posterior lumbar fusion in the treatment of lumbar degenerative diseases? World J Clin Cases 2020; 8: 5496-5500.

[8] Lee SH, Seol A, Cho TY, Kim SY, Kim DJ and Lim HM. A systematic review of interspinous dynamic stabilization. Clin Orthop Surg 2015; 7: 323-329.

[9] Wu AM, Zhou Y, Li QL, Wu XL, Jin YL, Luo P, Chi YL and Wang XY. Interspinous spacer versus traditional decompressive surgery for lumbar spinal stenosis: a systematic review and meta-analysis. PLoS One 2014; 9: e97142.

[10] Du MR, Wei FL, Zhu KL, Song RM, Huan Y, Jia B, Gu JT, Pan LX, Zhou HY, Qian JX and Zhou CP. Coflex interspinous process dynamic stabilization for lumbar spinal stenosis: long-term follow-up. J Clin Neurosci 2020; 81: 462-468.

[11] Shen HK, Fogel GR, Zhu J, Liao ZH and Liu WQ. Biomechanical analysis of different lumbar interspinous process devices: a finite element study. World Neurosurg 2019; 127: e1112-e1119.
[12] Zhao H, Duan LJ, Gao YS, Yang YD, Zhao DY, Tang XS, Hu ZG, Li CH, Chen SX, Liu T and Yu X. Comparison of two FDA-approved interspinous spacers for treatment of lumbar spinal stenosis: Superion versus X-STOP-a meta-analysis from five randomized controlled trial studies. J Orthop Surg Res 2018; 13: 42.
[13] Wilke HJ, Rohlmann F, Neidlinger-Wilke C, Werner K, Claes L and Kettler A. Validity and interobserver agreement of a new radiographic grading system for intervertebral disc degeneration: Part I. Lumbar spine. Eur Spine J 2006; 15: 720-730.
[14] Najarian S, Dargahi J and Heidari B. Biomechanical effect of posterior elements and ligamentous tissues of lumbar spine on load sharing. Biomed Mater Eng 2005; 15: 145-158.
[15] Lo HJ, Chen HM, Kuo YJ and Yang SW. Effect of different designs of interspinous process devices on the instrumented and adjacent levels after double-level lumbar decompression surgery: a finite element analysis. PLoS One 2020; 15: e0244571.
[16] Fan YP, Zhou SB, Xie T, Yu ZF, Han X and Zhu LL. Topping-off surgery vs posterior lumbar interbody fusion for degenerative lumbar disease: a finite element analysis. J Orthop Surg Res 2019; 14: 476.
[17] Xiao ZT, Wang LY, Gong H and Zhu D. Biomechanical evaluation of three surgical scenarios of posterior lumbar interbody fusion by finite element analysis. Biomed Eng Online 2012; 11: 31.
[18] Yue ZJ, Liu RY, Lu Y, Dong LL, Li YQ and Lu EB. Middle-period curative effect of posterior lumbar intervertebral fusion (PLIF) and interspinous dynamic fixation (Wallis) for treatment of L45 degenerative disease and its influence on adjacent segment degeneration. Eur Rev Med Pharmacol Sci 2015; 19: 4481-4487.
[19] Welton L, Krieg B, Trivedi D, Netsanet R, Wessell N, Noshchenko A and Patel V. Comparison of adverse outcomes following placement of superion interspinous spacer device versus laminectomy and laminotomy. Int J Spine Surg 2021; 15: 153-160.
[20] Wilke HJ, Drumm J, Haussler K, Mack C, Steudel WI and Kettler A. Biomechanical effect of different lumbar interspinous implants on flexibility and intradiscal pressure. Eur Spine J 2008; 17: 1049-1056.
[21] Pan H, Chen B and Deng LF. Biomechanical effects of the Coflex implantation on the lumbar spine. A nonlinear finite element analysis. Saudi Med J 2010; 31: 1130-1136.
[22] Lo CC, Tsai KJ, Chen SH, Zhong ZC and Hung CH. Biomechanical effect after Coflex and Coflex rivet implantation for segmental instability at surgical and adjacent segments: a finite element analysis. Comput Methods Biomech Biomed Engin 2011; 14: 969-978.
[23] Ma XL, Zhao XW, Ma JX, Li F, Wang Y and Lu B. Effectiveness of surgery versus conservative treatment for lumbar spinal stenosis: a system review and meta-analysis of randomized controlled trials. Int J Surg 2017; 44: 329-338.
[24] Huang WM, Chang ZQ, Zhang JT, Song RX and Yu XC. Interspinous process stabilization with Rocker via unilateral approach versus X-Stop via bilateral approach for lumbar spinal stenosis: a comparative study. BMC Musculoskelet Disord 2015; 16: 328.
[25] Wan ZM and Li GA. X-Stop(R) implantation effectively limits segmental lumbar extension in-vivo without altering the kinematics of the adjacent levels. Turk Neurosurg 2015; 25: 279-284.
[26] Wan ZM, Wang SB, Kozanek M, Passias PG, Mansfield FL, Wood KB and Li GA. Biomechanical evaluation of the X-Stop device for surgical treatment of lumbar spinal stenosis. J Spinal Disord Tech 2012; 25: 374-378.